MPC for dynamic power management of a grid supporting energy production hub with coupling reactance

Linde, Frederic; Torres, José Luis Rueda; Trivella, Alessio; Aarts, Ronald G.K.M.

DOI
10.1109/PowerTech59965.2025.11180485

Publication date
2025

Document Version
Final published version

Published in
2025 IEEE Kiel PowerTech, PowerTech 2025

MPC for dynamic power management of a grid supporting energy production hub with coupling reactance

Frederic Linde[1,2], *Member, IEEE,* José Luis Rueda Torres[2], *Senior Member, IEEE,* Alessio Trivella[3], and Ronald G. K. M. Aarts[1]

2025 IEEE Kiel PowerTech | 979-8-3315-4397-6/25/$31.00 ©2025 IEEE | DOI: 10.1109/PowerTech59965.2025.11180485

***Abstract*—Energy production hubs are emerging as a solution to stabilize power grids that are increasingly being challenged by renewable energy sources. The deployment of grid-forming inverters (GFMIs) inherently involves grid regulation tasks such as voltage and frequency control. Such control is distinctly advantageous over the passive grid-following inverter. GFMIs can actively stabilize the grid, but their introduction necessitates a coupling reactance to facilitate voltage and current control. Autonomous voltage and frequency control requires real-time coordination. However, applying MPC is complex due to the multiscale nature of the control problem. To overcome these challenges, this paper proposes a combined controller-hub design where a three-layer hierarchical MPC scheme controls an energy production hub comprised of an integrated energy storage system, a wind turbine, and a GFMI. By decomposing the problem into three distinct layers, the upper two layers can operate in non-real time and require only the bottom layer to work in real time. By designing the middle layer with a novel approach, we investigate how the coupling reactance dynamics affect the power setpoint determination of the energy production hub. The goal is to facilitate control over the grid's active and reactive power flows, voltage, and frequency. As the angle-based droop control law governs the coupling reactance dynamics, we study its incorporation into the MPC objective function and its effect on frequency stability. A simulation study shows how the droop control element alters the power setpoints in the middle layer to compensate for such frequency fluctuations. The results suggest that the hub and controller can reliably provide power from an uncontrolled, sustainable source while providing local stability to the energy grid.**

***Index Terms*—hierarchical model predictive control, energy production hub, steady-state target optimization, coupling reactance, power management, angle-based droop control**

NOMENCLATURE

ΔP	Small signal variation of P
δ_p	Relative phase angle across coupling reactance
η	Inverter efficiency
dP_{set}	Predicted supply-demand mismatch at PCC
E	Voltage at inverter terminal
P	Active power flow across coupling reactance
P_w	Wind power produced
$P_{0,set}$	Predicted demand at PCC
P_{ESS}	Power flow of ESS
$P_{grid,meas}$	Power measurement at PCC
$P_{inv,des}$	Setpoint variable at inverter terminal
P_{inv}	Power flow at inverter terminal
P_{loss}	Summed power losses
P_{RES}	Power flow on the main RES bus
P_{set}	Power setpoint at PCC
$P_{supply,pred}$	Predicted supply of P_w
PCC	Point of common coupling
RES	Renewable energy source
V	Voltage at PCC
w_{SOC}, w_1, w_2	Optimization weights
X_L	Ideal coupling inductance

[1] EEMCS Department, University of Twente.
[2] EEMCS Department, University of Delft.
[3] IEBIS Group, University of Twente.
E-mail: frederic.linde@kit.edu

I. INTRODUCTION

The transition to a sustainable energy landscape relies heavily on the use of renewable energy sources. Such emission-free means of energy production have the caveat that their output levels cannot be controlled. Unknown variations in production quantities give rise to a vast supply-demand mismatch. The mismatch can become problematic for several reasons.

As the European energy demand is projected to rise, grid overloads can become problematic. Especially the long-range transmission of electricity to consumer centers can lead to grid congestion and vast losses. Oppositely, prolonged underproduction can result in a severe supply deficit. For example, by 2050, the Netherlands expects to cover 75% of its electricity consumption with energy from offshore wind turbines [1]. Such low production diversification bears risks. The North Sea experiences frequent wind droughts, exposing weaknesses in power security and leaving people and the industry vulnerable.

Another conundrum is contingency cases. Algorithms in response to such cases must have rapid response times and have the capacity to accommodate drastic output changes. Regulations demand turbine output changes of $\sim$0.5 pu to occur within merely 2s [2]. Meanwhile, dynamic changes and disturbances on the grid have been estimated to have a frequency of around 10Hz [3].

Rapid current changes can be detrimental to sensitive equipment and its regulators. Necessary measures have downstream effects at the point of common coupling (PCC) and the wider grid. Compensatory control requires active and reactive adjustments in power flow, frequency, and voltage.

Consequentially, their cumulative effect can destabilize the grid. Therefore, many renewable energy sources cannot go online. Commonly deployed grid-following inverters are passive components and cannot participate in grid stabilizing tasks. Introducing a grid-forming inverter (GFMI) and coupling reactance enables control over the grid's variables, stabilizing the grid actively. Their addition potentially improves the grid's safety and operational efficiency. Part of the improvement relies on predictions of changes in supply and demand quantities.

Model predictive control (MPC) offers a widely used approach to controlling moderately complex multivariable systems. It optimizes control actions while considering predictions of different lengths and component degradation. Ensuring operational safety, the MPC can devise control signals while maintaining critical safety limitations [4]. However, the large range in system dynamics, predictions, and disturbances vastly increases computation time and deteriorates the solution accuracy. This circumstance is especially problematic in real-time computing as a system's short clock cycles must be complied with. With computation time as a constraint, plant models are often linearized. As a result, the control problems can be formulated as a linear programming routine and be solved efficiently. However, the linearization approach introduces a plant-model mismatch, potentially causing large gaps in optimality [5].

The singular perturbation theory can be employed to decompose such a complex multi-timescale problem [6]. Decomposition is achieved by introducing multiple MPC control layers that are temporally and functionally distinct. The separation of time scales significantly reduces the computational burden while minimizing losses in optimality [7].

So far, various literature sources (e.g. [8, 9]) have investigated a hierarchical MPC structure with two stages. They typically comprise a global nonlinear optimization (GNO) scheme and a linear optimizer that tracks the setpoint defined by the GNO layer. These sources, however, raise concerns regarding the reachability of setpoints determined in the GNO layer. As their feasibility spaces differ, the linear optimizer may not be able to reach a given setpoint. Similarly, optimization with a linear programming routine has been found to overestimate cost significantly compared to a nonlinear problem, which, on the other hand, was found to be computationally more costly to solve [5].

Negenborn *et al.* ([10]) showed improved voltage stability of a simulated grid by introducing a supervisory MPC layer to provide setpoints to the primary control layer. [4] examine the introduction of an intermediary layer to the hierarchical MPC scheme from a control theoretical perspective. They show that a steady-state target optimization layer (SSTO) of quadratic form improves the setpoints' optimality.

This paper converges existing work from the control theory with the energy production hub application. The issues raised in the application can be approached by introducing a 3-stage MPC. With improved performance shown in control theory, this scheme is hypothesized to complement a designed energy production hub. The hub comprises a wind turbine, an integrated energy storage system (ESS), and a GFMI. The ESS integrates an H_2 cycle, a battery (BESS), and a supercapacitor (SC). Review papers (such as [11]) have not reported on this storage system and control structure combination.

Section II proposes a 3-stage hierarchical MPC, leveraging the singular perturbation theory. It is designed congruently with an energy production hub that complements the control design, proposing a novel integrated approach. The control aspect focuses on the middle layer of the three stages. As 2-stage MPC solutions have been investigated in the hub context, the design of the newly added SSTO layer under consideration of the ESS is of interest. Therefore, after presenting the novel controller-hub concept, the focus is on the mathematical formulation of the SSTO layer in objective function form. The layer itself is formulated considering the coupling reactance. Herein, it newly implements the droop control law in objective function form. Section III presents the mathematical formulation of the SSTO layer, where equations are rewritten to fit the objective function form of the middle layer. Building on droop-based control approaches ([12–15]), this model aims to provide frequency stability by altering the synthesized power setpoint. Finally, section IV presents the simulation results, and conclusions are drawn in section V.

II. Hub and control concept

The application goal is to deploy inverter-based renewable energy sources at industrial scale. By introducing intermediary energy storage and advanced control methods, uncertain means of energy production can be incorporated to respond to a dynamic demand. Their grid-stabilizing properties enable independent entities to deploy and manage assets decentrally, necessitating only limited information exchange with the grid operator.

The energy production hub concept and control strategy pair the elements within the energy production hub with a respective MPC layer. This way, each layer can take control action based on its prediction.

A. Hub concept

As intermediary energy storage is integral to optimal power flow management, Fig.1 proposes an energy production hub design that complements a controller in delivering demanded power quantities. The integrated ESS aims to compensate for supply-demand mismatches ranging from several months to fractions of seconds. The H_2 cycle is geared towards handling seasonal variations, and prolonged events like a wind drought. The BESS compensates for intra-day supply-demand mismatches. The SC is intended to deal with rapid sub-second changes in grid loading, stabilizing the grid's frequency and adding virtual inertia.

Apart from the storage, a wind turbine acts as the prime mover of the hub. A grid-forming inverter (GFMI) establishes the connection to the general grid via the point of common coupling (PCC). It synthesizes the 3-phase power, synchronizing it with the grid's power flow. All components were sized to match the power and voltage rating of the wind turbine.

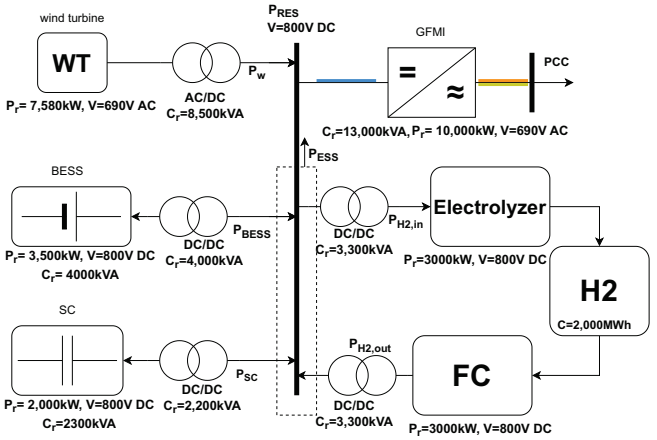

Figure 1: Schematic overview of the components of the energy production hub.

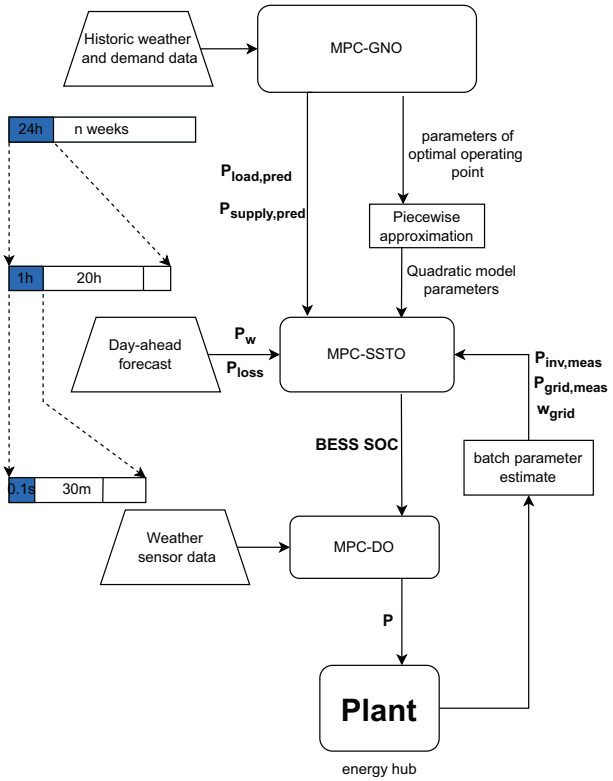

Figure 2: Flowchart showing the controller stages and their interaction. The update cycle of the receding horizon scheme can be seen on the left, showing each prediction horizon and control step.

B. Control concept

As illustrated in Fig.2, each control layer integrates a storage element by determining the state of charge setpoints. Assuming they operate on distinct, non-overlapping time scales, one can ascribe functionality to each layer. The global nonlinear optimization (GNO) layer's goal is to determine an operating point for the next layer. The operating point is then quadratically approximated to simplify the control signal to estimate optimization parameters that describe the steady state target optimization (SSTO) layer. It determines power and SOC setpoints on the hub side to optimize the power flow to the grid. It comprises a quadratic objective function and linear constraints. The synthesized setpoints are finally passed to the dynamic optimization (DO) layer. It directly controls the power flow of the storage components. This lower layer is formulated with a linear objective function and constraints. By leveraging the singular perturbation theory, the MPC structure can perform real-time and non-real-time computing. This way, only the DO layer must run in real time, alleviating the time constraints on the other two layers. They can be updated less frequently and perform more time-intensive computations. Fig.2 also shows an exemplary prediction horizon scheme. The operating point and setpoints are passed down to the next layer, shortening the horizon and simplifying the computation. The longer-term predictions are now considered implicitly. Here, it should be assumed that the linear programming routine of the DO layer can be solved within the real-time constraints.

C. SSTO layer

Building on the literature that investigated 2-stage MPC structures, the first step is the mathematical formulation of the SSTO layer. It links the GNO and the DO layers by devising linear setpoints from a nonlinear operating point. The quadratic objective function was chosen for two reasons. Firstly, [4] found an improvement in optimality from the consequent setpoint determination, and secondly, because the accuracy of a quadratic approximation is higher than that of a linear one. To limit the scope of this work, the interaction with the other layers is assumed, such that the quadratic approximation is known and the devised setpoints are linear. It meets the requirements of the SSTO layer in the complete structure.

Due to its function, the modeling focus is set on the SSTO layer. It manages the power balance between the production unit, the storage, and the grid. Further, the quadratic form reduces the mismatch between the GNO and DO layers. It can minimize issues stemming from the uncertainty associated with their direct interaction, effectively relieving feasibility issues and improving solution accuracy [4, 16].

Successful deployment of such an integrated energy production hub depends on an active stability contribution to the grid. Such a task must be achieved via a GFMI. Thus, the control concept must be able to regulate the active and reactive power flow. It must also stabilize the grid's voltage and frequency.

Introducing a coupling reactance between the GFMI and the PCC enables the decoupling of the active and reactive power flows. Leveraging the droop control scheme, their control is much facilitated. The following modeling approach details how the active droop control is reformulated to fit the objective function form of the SSTO layer, providing power and frequency stability. Thus, added to the proposed formulation are the coupling reactance equations and droop

control law.

III. Proposed MPC structure

This section discusses how the mathematical formulation of the middle layer, the non-real-time SSTO layer, was performed. Its objective function and constraints comprise five elements that describe how electrical power flow equations are captured in an MPC scheme.

A. Proposed objective function

The non-smooth quadratic objective function aims to minimize the error between the desired inverter setpoint $P_{inv,des}$ and the measured power flow $P_{inv,meas}$. It determines a value for its optimization variable P_{inv}, aiming to optimize the storage's SOC while meeting the predicted demand $P_{load,pred}$.

$$\begin{aligned}\min_{k\in K} \quad & w_1|P_{inv,err}(k)| + w_2(P_{inv,err}(k))^2 + \\ & w_{SOC}(SOC_{ESS}(k) - SOC_{ESS,des})^2\end{aligned} \tag{1}$$

The weights w_{SOC}, w_1, and w_2 tune the square term of the SOC and the linear and square terms of the objective function, respectively. After initialization, they were adjusted manually. The process followed the goal of minimizing the absolute function value and the necessary condition of optimality. After tuning, the weights were kept constant to diminish their influence on the simulation results. The prediction horizon spans $K = 20$ time steps in hours. All time series values have according dimensions of $[1, K]$. The third term minimizes the weighted square error between optimization variable SOC_{ESS} and its setpoint $SOC_{ESS,des}$. Composing the power setpoint are measured and predicted quantities.

$$\begin{aligned}P_{inv,err}(k) &= P_{inv,des} - P_{inv}(k) \\ P_{inv,des} &= \lambda P_{inv,meas} + (1-\lambda)P_{inv,pred}\end{aligned} \tag{2}$$

Here, $\lambda \in [0, 1]$ balances the influence of the predicted and measured inverter setpoint on the solution. They are both arrays of format $[1, K]$. Using power continuity, the prediction term comprises the anticipated power flow $P_{load,pred}$ to meet the demand at the PCC and the expected variation in power flow that compensates for frequency fluctuations.

$$P_{inv,pred} = P_{load,pred} + \Delta P \tag{3}$$

B. Constraint: Power balance equation

The constraints in the power balance equation manage the power flow between the production unit, the storage, and the main bus that connects the hub to the grid (Fig.1).

$$\begin{aligned}P_w - P_{ESS}(k) - P_{loss} &= P_{RES}(k) \\ \eta P_{RES}(k) &= P_{inv}(k) \\ P_{ESS}(k) = P_{BESS}(k) + P_{SC}(k) &+ P_{H_2}(k) \\ P_{H_2}(k) &= P_{H_2,in}(k) - P_{H_2,out}(k)\end{aligned} \tag{4}$$

where P_w is the power produced by the wind turbine, P_{ESS} describes the power flow into and out of the integrated storage, and P_{loss} are the summed losses of the components on the hub side. P_{RES} is the power flow on the main hub bus. It is connected to the grid via the inverter as P_{inv} on the grid side. Inverter losses are captured by the efficiency term η. $P_{H2,in}$ and$P_{H2,out}$ are the respective power flows into the electrolyzer and the fuel cell.

C. Constraint: ESS update law

The following constraint from [17] integrates P_{ESS} to determine the state of charge (SOC) of the ESS. With this term, it is possible to constrain the SOC explicitly.

$$\begin{aligned}SOC_{ESS}(k+1) &= SOC_{ESS}(k) + P_{ESS}(k) \\ SOC^L_{ESS} \le SOC_{ESS}(k) &\le SOC^U_{ESS}\end{aligned} \tag{5}$$

The term is the update law, adjusting the new SOC by the power flow in and out of the ESS. Lastly, $SOC^L_{ESS} = 0.1$ and $SOC^U_{ESS} = 0.9$ are the hard constraints on the lower and upper SOC respectively.

D. Constraint: Droop control

The expression for the droop control is derived to determine power flow variations in the coupling reactance between the hub and the grid. The inverter itself is assumed to be ideal.

Firstly, the general expression for power flowing across a reactance is approximated by constraining the maximum power angle $\delta_{P,max} = 30°$ [15]. Imposing this constraint limits the amount of reactive power delivered which can be done without loss of generality. Operating in this quasi-linear region achieves decoupling the two expressions with a 4% error at maximum value [12].

$$P = \frac{EV}{X_L} sin(\delta_P) \approx \frac{EV}{X_L}\delta_P \tag{6}$$

The active power expression poses a challenge as it requires the error-prone integration of the power angle. The next step is performed as in [13] and utilizes the small signal variation of the coupling reactance's power flow around the operating point, such that

$$\Delta P = \frac{EV}{X_L}\Delta\delta_P \tag{7}$$

This expression enables the use of direct angular velocity measurements, such that $\Delta\delta_P = \omega_{inv} - \omega_{grid}$ and permits the addition of the droop control law

$$\omega_{inv} = \omega_0 + m_P(P_{set} - P_{grid,meas}) \tag{8}$$

to compensate for deviations based on anticipated and measured power flow. The droop gain values were obtained from [14]. Dissection of the setpoint variable into its nominal value and variation yields $P_{set} = P_{0,set} + dP_{set}$. $P_{0,set}$ can be obtained as the operating point from the GNO layer by taking $P_{0,set} = P_{load,pred}$ (Fig.2). It is essentially a prediction of the demand quantities on the grid. Ideally, this demand should equal the supply. Realistically, they are rarely equal, such that $dP_{set} = P_{supply,pred} - P_{load,pred}$, predicts the supply-demand mismatch. Now, considering frequency variations, the entire expression for the variation in the power flow of the coupling reactance becomes:

$$\begin{aligned}\Delta P &= \frac{EV}{X_L}(\omega_0 - \omega_{grid} + P_f) \\ P_f &= m_P(P_{load,pred} + dP_{set} - P_{grid,meas})\end{aligned} \tag{9}$$

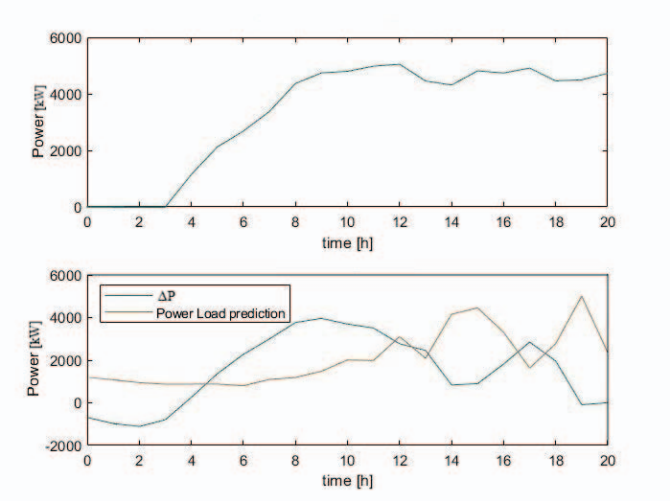

Figure 3: Power production of the turbine (top) and prediction of the load as well as the adjustment due to the reactance (bottom).

IV. Results

The optimization problem formulated for the SSTO layer is implemented in MATLAB R2023b (i7-11800H @ 2.30GHz, 32GB RAM). Using its fmincon solver, solutions approximating the optimal control are calculated. The external grid is assumed to be stable with a constant voltage. The computation time for this optimization was in the order of multiple seconds. To stabilize the voltage and frequency in real-time, a control step may only take 10-100ms. This discrepancy highlights the benefit of the hierarchical MPC because only the lowest layer must operate in real-time. This way, the SSTO layer can perform more complex computations without critical time constraints. Due to the research focus, the DO layer was explicitly excluded from the simulations where critical hardware constraints don't affect the operation of the SSTO layer.

The produced quantities and the resulting power flow across the coupling reactance are plotted in Fig.3. The wind turbine's power output is determined by assuming a Gaussian distribution of a wind profile in the North Sea. The load on the grid side is based on aggregated measurements from yearly household energy consumption [18]. ΔP depicts the power flow across the inverter under consideration of frequency variations.

Fig.4a shows the power flow and SOC of the ESS. Its power flow is actively controlled in response to supply-demand mismatches between the turbine and the grid.

Depicted in Fig.4b are the synthesized setpoint at the inverter terminal and the power flow following the setpoint. Setpoint changes govern the inverter power flow as they react to changes in frequency power. Their correlative relationship can be attributed to changes of ΔP, altering the flow at the inverter due to frequency adjustments.

Optimization weight variations showed how the power setpoint tracking is related to the SOC. Increasing weights

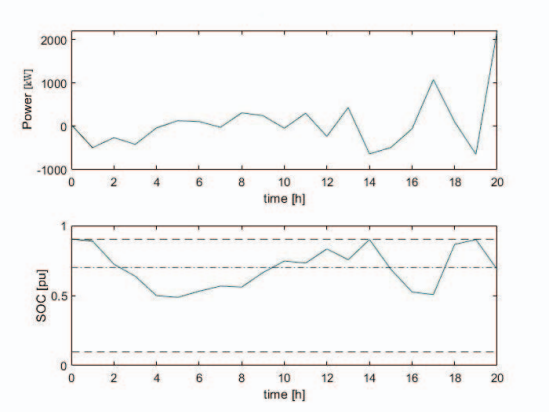

(a) Power flow (top) and SOC (bottom) of the ESS.

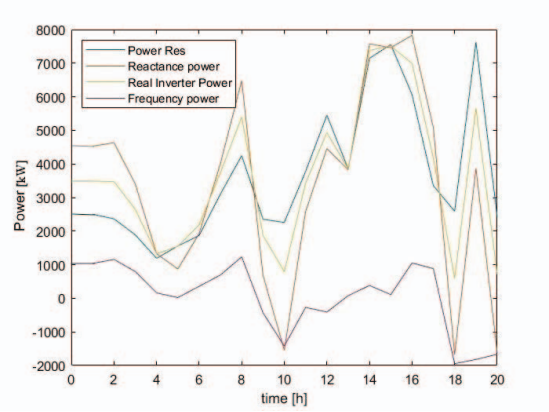

(b) Referring to Fig. 1: Active power flow: Power Res (blue) is the power flow on the main bus on the hub side. Reactance power (orange) is the power setpoint after the inverter and Real inverter power (yellow) is the actual power flow. Frequency power (purple) is the share of the total power that flows due to changes in grid frequency.

Figure 4: Results of the optimization with a frequency optimization variable included.

w_1 or w_2 resulted in higher tracking accuracy and greater deviations from the desired SOC. Increasing w_{SOC} had the opposite effect. They enable balancing competing objectives within the optimization function.

The simulation details how the power flow ΔP across the coupling reactance is adjusted due to power fluctuations on the grid. Decoupled control demonstrates effective active power flow management. The energy produced by the wind turbine is buffered by the energy storage system and released in response to active power demand on the grid.

The results show how the droop control term can be leveraged to counter frequency fluctuations. Due to the droop control term, the control performs dynamic adaptions under consideration of frequency fluctuations. Power flow adjustments at the inverter terminal are made in response to the grid.

V. Conclusion

This paper combined two key aspects that contributed to renewable energy integration: the conceptual controller-hub design and the droop control integration into the SSTO layer.

Considering the coupling reactance and droop control, the SSTO determines power and SOC setpoints on the hub side to ensure a steady power supply to the GFMI. With it, the control structure can actively support the grid by influencing the active power flow. The droop control element makes power adjustments based on frequency fluctuations.

Hierarchical MPC control, in conjunction with the decoupled droop control, provides an integrated solution for managing the frequency and power flow in a grid-supportive manner. Here, the key component is the coupling reactance, which links an energy production hub with the grid in a manner that has not been studied before. Due to the locally stabilizing effect, augmenting renewable energy sources to energy production hubs enables their decentral connection to the energy grid without compromising safety.

One aspect for further investigation would be the addition of the reactive power droop control law into the SSTO layer. The translation of the inverter setpoint Q to the hub side setpoints would be of interest. Active control of the inverter's power angle influences the grid dynamics and the hub's power flow. With control of the reactive power flow, one can examine the influence of cross-coupling effects on the control. Although the dynamic optimization (DO) layer is conceptually outlined, further work is needed to specify its problem formulations and validate its performance in real-time. A comparative study with traditional control methods will be part of future work.

References

[1] Rijksoverheid, "Offshore wind energy," Rijksoverheid, 2023. [Online]. Available: https://www.government.nl/topics/renewable-energy/offshore-wind-energy.

[2] M. Knechtges and A. Moser, "Impact of grid-forming control and the available energy in dc links on the system frequency after a system split," in *2022 IEEE 7th Southern Power Electronics Conference (SPEC)*, 2022, pp. 1–5. DOI: 10.1109/SPEC55080.2022.10058233.

[3] Y. Huang *et al.*, "Modeling and stability analysis of dc-link voltage control in multi-vscs with integrated to weak grid," *IEEE Transactions on Energy Conversion*, vol. 32, no. 3, pp. 1127–1138, 2017. DOI: 10.1109/TEC.2017.2700949.

[4] A. G. Marchetti, A. Ferramosca, and A. H. González, "Steady-state target optimization designs for integrating real-time optimization and model predictive control," *Journal of Process Control*, vol. 24, pp. 129–145, 1 Jan. 2014, ISSN: 09591524. DOI: 10.1016/j.jprocont.2013.11.004.

[5] K. A. Pruitt, R. J. Braun, and A. M. Newman, "Evaluating shortfalls in mixed-integer programming approaches for the optimal design and dispatch of distributed generation systems," *Applied Energy*, vol. 102, pp. 386–398, 2013. DOI: 10.1016/j.apenergy.2012.07.030.

[6] P. Tatjewski, "Advanced control and online process optimization in multilayer structures," *Annual Reviews in Control*, vol. 32, pp. 71–85, 1 Apr. 2008, ISSN: 13675788. DOI: 10.1016/j.arcontrol.2008.03.003.

[7] M. H. Holmes, *Introduction to Perturbation Methods*. Springer, 1995, ISBN: 978-0-387-94203-2.

[8] R. Scattolini, *Architectures for distributed and hierarchical model predictive control - a review*, May 2009. DOI: 10.1016/j.jprocont.2009.02.003.

[9] R. R. Negenborn, S. Leirens, B. D. Schutter, and J. Hellendoorn, "Supervisory nonlinear mpc for emergency voltage control using pattern search," *Control Engineering Practice*, vol. 17, pp. 841–848, 7 Jul. 2009, ISSN: 09670661. DOI: 10.1016/j.conengprac.2009.02.003.

[10] R. R. Negenborn *et al.*, "Supervisory hybrid model predictive control for voltage stability of power networks," *American Control Conference*, May 2007. DOI: 10.1109/ACC.2007.4282264. [Online]. Available: http://psdyn.ece.wisc.edu/IEEEbenchmarks/.

[11] A. Maroufmashat, S. T. Taqvi, A. Miragha, M. Fowler, and A. Elkamel, *Modeling and optimization of energy hubs: A comprehensive review*, Sep. 2019. DOI: 10.3390/inventions4030050.

[12] J. H. Eto *et al.*, "The certs microgrid concept, as demonstrated at the certs/aep microgrid test bed," 2018. [Online]. Available: https://api.semanticscholar.org/CorpusID:173172513.

[13] M. Moritz *et al.*, "Distributed model predictive frequency control of inverter-based power systems," *IEEE Access*, vol. 12, pp. 53 250–53 265, 2024. DOI: 10.1109/ACCESS.2024.3387369.

[14] M. J. Erickson and R. H. Lasseter, "Integration of battery energy storage element in a certs microgrid," in *2010 IEEE Energy Conversion Congress and Exposition*, 2010, pp. 2570–2577. DOI: 10.1109/ECCE.2010.5617986.

[15] R. H. Lasseter and P. Piagi, "Control and design of microgrid components," University of Wisconsin, Jan. 2006, p. 257.

[16] D. Krishnamoorthy, B. Foss, and S. Skogestad, "Steady-state real-time optimization using transient measurements," *Computers and Chemical Engineering*, vol. 115, pp. 34–45, Jul. 2018, ISSN: 00981354. DOI: 10.1016/j.compchemeng.2018.03.021.

[17] J. LeSage, *Microgrid energy management system (ems) using optimization*, 2024. [Online]. Available: https://github.com/jonlesage/Microgrid-EMS-Optimization/releases/tag/v19.1.0.

[18] J. Bendík, "Dataset of 15-minute values of active and reactive power consumption of 1000 households during single year," *Mendeley Data*, vol. 2, 2023. DOI: 10.17632/pns69yxgrp.2.